Asia Pacific Research Initiative for Sustainable Energy Systems 2021 (APRISES21)

Office of Naval Research
Grant Award Number N00014-22-1-2045

Ocean Thermal Energy Conversion (OTEC) Heat Exchanger Development (November 2024 to July 2025)

Task 5

Prepared for
Hawaiʻi Natural Energy Institute

Prepared by
Makai Ocean Engineering

August 2025

HNEI
Hawaiʻi Natural Energy Institute
University of Hawaiʻi at Mānoa

MAKAI OCEAN ENGINEERING

ANNUAL REPORT

SUBCONTRACT MA2126

Prepared For

HAWAII NATURAL ENERGY INSTITUTE
1680 East West Road, POST 109
Honolulu, HI, 96822
USA

Prepared By

MAKAI OCEAN ENGINEERING
PO Box 1206, Kailua, Hawaii 96734

August 6, 2025

TABLE OF CONTENTS

LIST OF FIGURES

LIST OF TABLES

1. INTRODUCTION

Makai Ocean Engineering has been developing Thin Foil Heat Exchangers (TFHX) for use in seawater-refrigerant, air-water, and water-water applications. This report summarizes work performed between November 2024 – July 2025.

In this period, Makai's efforts included improving TFHX fabrication and assembly methods, characterization of TFHX thermal performance, and investigation of biofouling mitigation methods.

TFHX Design and Fabrication Development

Makai investigated options to improve the assembly process and gained experience with installation and operation of the cassette design. Makai continued to explore options to increase the internal fluid flow rates to make the TFHX more competitive in applications that already use plate-and-frame heat exchangers.

TFHX Characterization and Model Development

Makai performance tested two 2-MW_{th}, cassette-style seawater-ammonia TFHXs on the HX Test Facility. The condenser was tested in a horizontal counterflow configuration and the evaporator was tested in a vertical, cross-flow, falling film configuration. Evaporator performance met model predictions but the condenser underperformed, likely due to issues with assembly.

TFHX Prototype Construction and Demonstration

Makai developed several concept designs for an accessible seawater/seawater heat exchanger and selected one to proceed with construction. Makai also designed the test station (as part of the HX Test Facility) to prepare for demonstration and testing.

Long-Duration Biofouling and Intake Screen Testing

Makai continued the intake screen testing and concluded 3-mm plate spacing in-situ cleaning and baseline tests after 1 year. The cleaned unit had a 13% increase in pressure drop whereas the baseline unit had 400% increase in pressure drop. Makai developed a system to clean TFHX units with 2.12-mm plate spacings and began a new submerged test.

2. TFHX DESIGN AND FABRICATION

In this period, Makai's TFHX design efforts focused on commissioning and performance testing the 2-MW_{th} seawater-ammonia TFHXs and improvements to the assembly process.

2.1. CASSETTE DESIGN FOR REFRIGERANT HEAT EXCHANGERS

Makai previously reported on the design, construction (under separate funding), and installation of the cassette-style design for large-scale heat exchangers (Figure 1). In this period, Makai commissioned the heat exchangers and the newly upgraded HX Test Facility.

Figure 1. Cassette design

At high seawater flow rates, the plate stacks in both the evaporator and condenser were observed to shift (Figure 2). This was attributed to insufficient compression to hold the middle plates in place. The force of the seawater pushed the plates against and bent the manifold bolt nearest to the stack.

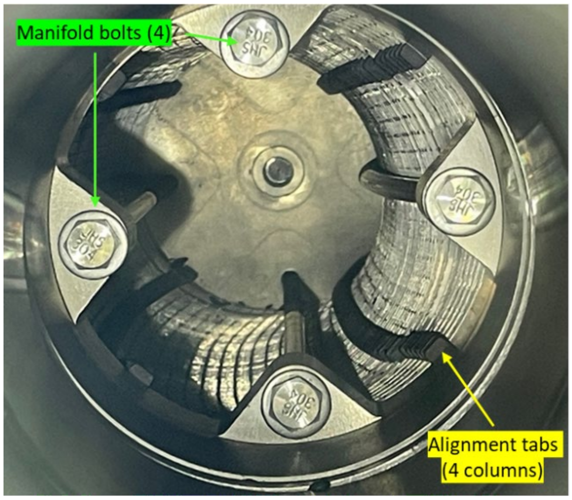

Figure 2. Plate shift viewed through manifold ports.

In the condenser, the exact flow rate associated with plate shift was not observed, but the maximum flow rate prior to the plate shift discovery was 1500 gpm. The condenser remained pressurized, indicating the plates did not move enough to lose the plate-to-plate seal. In the evaporator, plate shift was observed between 3000-3800 gpm and resulted in loss of sealing, as indicated by rapid depressurization on the ammonia side (Figure 3).

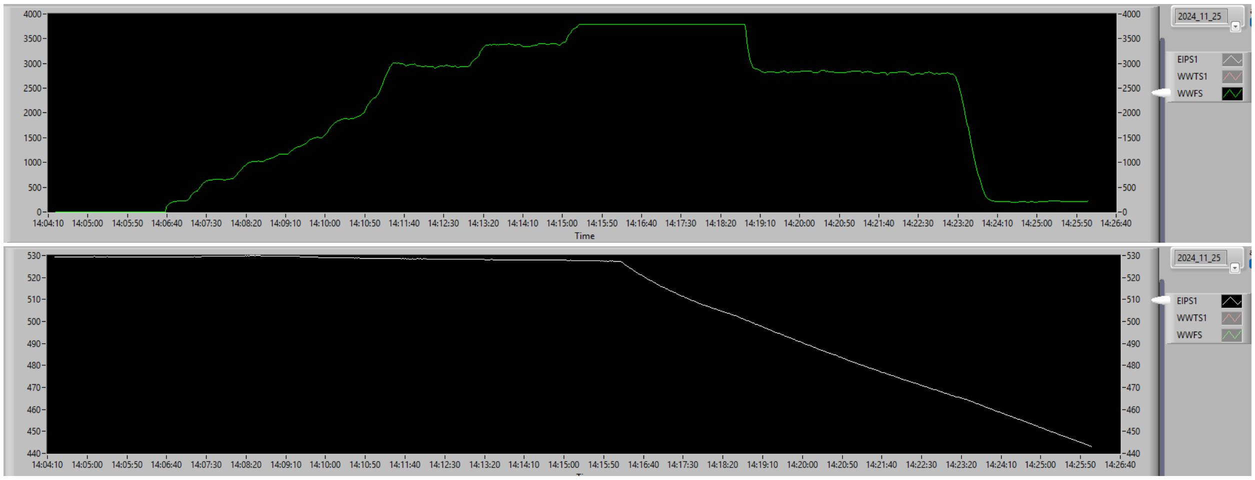

Figure 3. (top) Incrementally increasing warm seawater flow through the TFHX evaporator. (bottom) Depressurization on the ammonia side indicates a loss of sealing which coincides with plate shift that started between 3000-3800 gpm.

The current units were corrected by adding two plates to each stack in the evaporator to increase the compression (the condenser already had two additional plates per stack) and using a sleeve around the manifold bolts to limit the distance the stack can shift to prevent loss of sealing.

After the units were returned to service and initial performance testing was complete, an upstream event caused a sudden pressurization of the warm seawater side of the HX Test Facility which resulted in another evaporator leak. Upon removal and inspection, several plates had leaks in the transition zone, where rocks or shells had become wedged in. Makai suspects the repeated cycles of pressurization and depressurization on the seawater side allowed sharp debris (small rocks) to work its way in and become wedged between plates, particularly because internal channels in the transition zone are slightly larger. The sudden pressurization/depressurization event may have been sufficient to impact the plates against the debris and produce small pinholes. Furthermore, the Delrin header plate was warped, showing a 4-mm gap between the housing and header interface. Makai suspects this was caused by pressure imbalances between the plate stack and the header plate/housing interface; since the seawater channels in the plate are smaller, the plate stack is at a lower pressure compared to any voids that are filled/pressurized with seawater.

Future designs will address these lessons learned by using:

- Larger and/or stiffer manifold bolts to ensure compression is maintained.
- Physical stops to prevent plates from shifting.
- Updated header plates to use a different material and/or use fasteners to tie the header plate to the housing.

- Screens to prevent debris from getting lodged between the plate. Although there is a strainer on the warm seawater inlet to the HX Test Facility, whenever the strainer basket is lifted out to remove accumulated debris, some shells, rocks, and sand fall into the body of the strainer and get pushed through when seawater flow is restored. This issue is likely specific to the seawater distribution system at NELHA but Makai will evaluate options to install filters specific to the TFHX so the TFHX will be protected independently of the seawater distribution system.

With the current design, Makai has successfully demonstrated the concept and the procedure for removing and reinstalling a plate stack. Furthermore, the multiple (unplanned) events that required removal/re-installation cemented the importance of the removable plate stack.

2.2. INTERNAL PRESSURE DROP TESTING

In applications where the internal fluid has higher viscosity and/or density than ammonia, the TFHX faces the challenge of higher internal fluid pressure drop for the same flow rate compared to other plate-frame heat exchangers because the TFHX has smaller internal channels. While the TFHX can meet the same duty using lower internal flow rates and a larger temperature difference, it is unclear whether that is a viable solution in all applications for the equipment being cooled. Therefore, Makai has been developing designs that have lower internal pressure drops so the TFHX can be used as direct replacement rather than requiring substantial changes to the rest of the system.

Instead of building 6 plates, stacking them in a module, and installing the unit in the 100-kW Test Station, Makai constructed a single-plate pressure test station so individual plates can be tested. The first 3 tests were conducted on existing (i.e., already fabricated) plates.

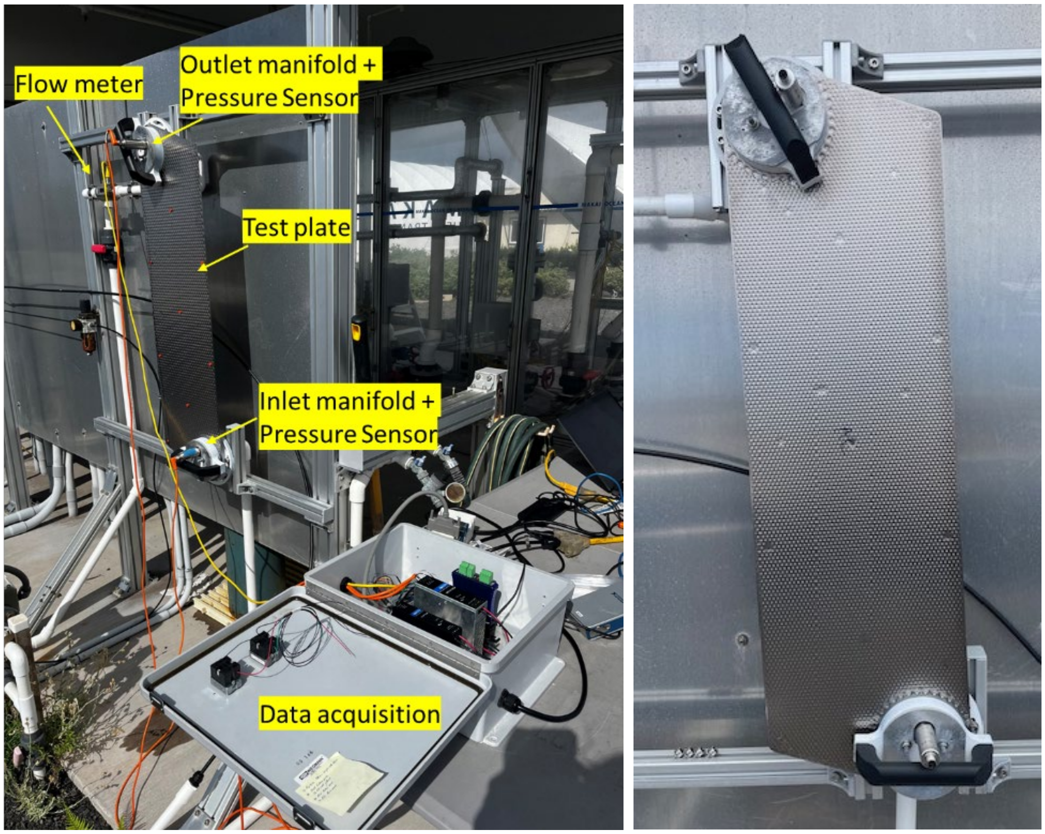

Figure 4. Single plate pressure test setup.

The effective internal channel sizes are 0.515mm, 0.616mm, and 0.678mm for AC, AB, and AA designs, respectively. In theory, the AA design should have a lower pressure drop than the AB design, however, the larger welds used in the AA pattern likely cause the fluid to accelerate and decelerate more to get around the welds compared to the smaller welds used in the AB pattern and contribute to the higher pressure drop for a larger effective channel. One additional area that requires additional examination is the effect of the transition zone. Makai's test plan for the next work period includes trying different transition zones and orientations for the pattern weld design.

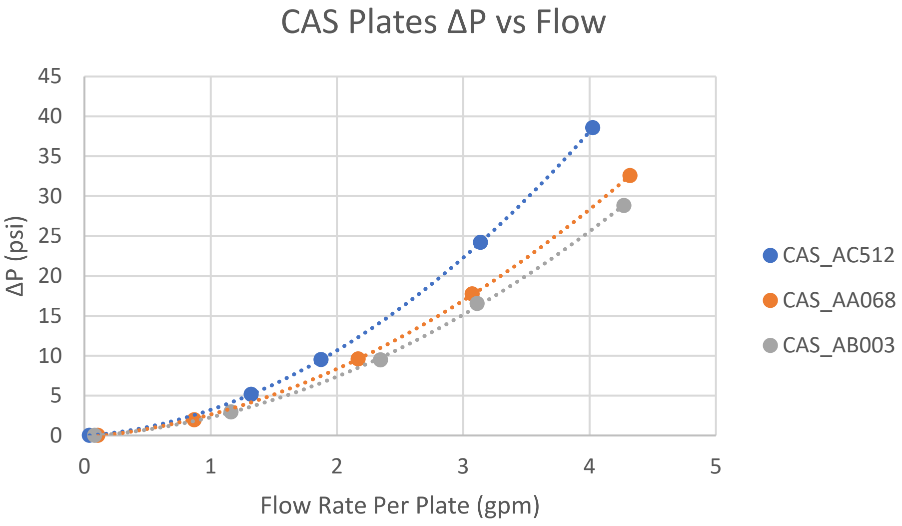

Figure 5. Single plate pressure drop test

2.3. PLATE FABRICATION IMPROVEMENTS

Under separately funded work, Makai designed a new High Speed Welding System (HSW 2.0). This new system is expected to reduce plate fabrication time. In addition to speeding up the fabrication process, Makai has used the lessons learned from prior work to design subsystems aimed at automating the process while improving the reliability and repeatability.

With the improvements in plate fabrication, housing costs have become a more significant contribution to the overall heat exchanger cost. Makai has been focused on cost-effective housing designs (see Section 4) as the next step in the TFHX commercialization pathway.

3. TFHX PERFORMANCE TESTING

In this period, Makai spent considerable effort commissioning, repairing, and re-commissioning the HX Test Facility for performance testing. The 2-MW$_{th}$ TFHX condenser and evaporator were tested in this period.

3.1. HX FACILITY COMMISSIONING AND REPAIRS

Makai completed upgrades to the HX Test Facility under separately funded work. Commissioning and subsequent repairs and re-commissioning were conducted under this contract.

The major issues and lessons learned from commissioning and operations are summarized in the following sections.

3.1.1. Ammonia System Cleanliness

System cleanliness specifications must be established for ammonia system piping. Both ammonia pumps were damaged when debris in the ammonia piping system got stuck in the pump internal components. Makai cleaned the piping sections that were welded on site with compressed air but was not able to clean the separator and buffer tank assemblies that were assembled off-site and installed as an assembly.

Both pumps seized during startup checks. Upon inspection, the amount of fine particles that passed through the filters at the pump inlets (Figure 6) combined with tight clearances of the pump design, led to damage on the interfacing surfaces of both pumps (gears, bearings, casing) (Figure 7 and Figure 8). The particles were removed and gouges were polished to the best of our ability and the pumps were re-assembled for operation. In addition, a finer mesh filter was added inside the existing filter.

Figure 6. Debris in ammonia piping caught in strainer.

Figure 7. Recirc pump damage.

Figure 8. Feed pump damage.

The initial repairs enabled an initial set of performance data collection with constant attention and servicing to the pumps. However, after 2 weeks, the pumps seized again and required an overhaul.

Inspection after 2-weeks of intermittent operations suggest that both debris and cavitation resulted in wear/grinding between the pump head and rotor. Large metal particles were also embedded in the pump head and suction side of the pump casing (Figure 9). The physical interference also contributed to bearing damage which then exacerbated the problem because the pump was no longer rotationally balanced and the wobbling caused more wear damage. Makai performed light polishing of the surfaces to remove interference and then replaced the bearings, which is a complex process requiring heating and dry ice. Both pumps were returned to service and have been mostly trouble-free during operations.

During the overhaul period, Makai installed a backflush line to use water to clean the piping from the feed pump outlet to the recirc pump inlet. Very little debris was flushed out (Figure 10); either most of the debris was already removed in the strainer at this point or the debris was generated by wear and/or cavitation within the pump.

Figure 9. Metal chunks embedded in the pump casing (left) and pump head (right).

Figure 10. Flushing the ammonia line between the feed pump outlet and recirc pump inlet did not remove significant amounts of shavings/debris.

In addition to pumps, system cleanliness affects valve seats. Makai initially checked that all the quick close valves sealed during commissioning. However, during an event where seawater was inadvertently drained from the condenser leading to an ammonia leak, the safety system shut the quick close valves to isolate the condenser but the quick close valve at the condenser exit (between the buffer tank inlet and condenser outlet) was found to leak. Makai found weld slag on sealing surfaces that interfered with the seal (Figure 11). Once repaired, the valve was verified to seal prior to returning to ammonia service.

Figure 11. Weld slag in valve seating surfaces prevent quick-close valve from sealing.

3.1.2. Ammonia Pump Selection

Separate from the issues with the pump seizing and requiring multiple servicing/overhauls, the recirc pump has difficulty providing adequate flow to target ~50% quality at high duties. The issue is exacerbated because the inlet piping to the evaporator is complex and contains an orifice flow meter to one cassette which increased the pressure drop (and lowers the flow). Makai suspects the pump performance was affected by small changes to the clearances due to polishing to remove embedded particles, gouges from the debris, and cavitation due to inadequate suction head ($\mathrm{NPSH_r}$).

These challenges are due to the requirements of a test facility compared to an operational system. In a test facility, pumps must operate over a wide range of flow rates and pressure drops to characterize and identify optimal performance points. Makai wanted to use gear pumps or positive displacement pumps because there is a wider range of flow control using VFDs compared to centrifugal pumps. The previous facility used centrifugal pumps and a complex system of three control valves and bypass lines was required to control feed and recirc flow rates. An operational OTEC system is expected to have a narrow range of flow rates and pressures, making pump selection easier and centrifugal pumps may still be considered.

3.1.3. Seawater System Cleanliness

Commissioning activities for the warm seawater system were performed using the CHART heat exchanger to limit the amount of "stuff" that could get stuck on the leading edge of the TFHX plate stack. However, there were still sections of piping unique to the TFHX that could not be cleared separately. Additionally, each time the warm seawater strainer basket was emptied, some amount of sand, shells, and marine debris would fall out and into the bottom of the inlet piping and eventually carried through the rest of the system to the inlet of the TFHX.

Makai suspects the plate shift event described in Section 2.1 was partially due to debris clogging the inlet face/leading edge of the evaporator plate stack. This increased pressure difference led to some loss of compression and the plates in the middle of the stack were pushed out of alignment.

Instead of relying on pressure drop, Makai installed three viewports to observe the evaporator inlet face during operations and a backflush to remove some of the debris without having to remove the evaporator. The viewports also allowed access to manually brush the leading edges. Neither backflushing or brushing were 100% effective but was enough to complete initial performance data collection.

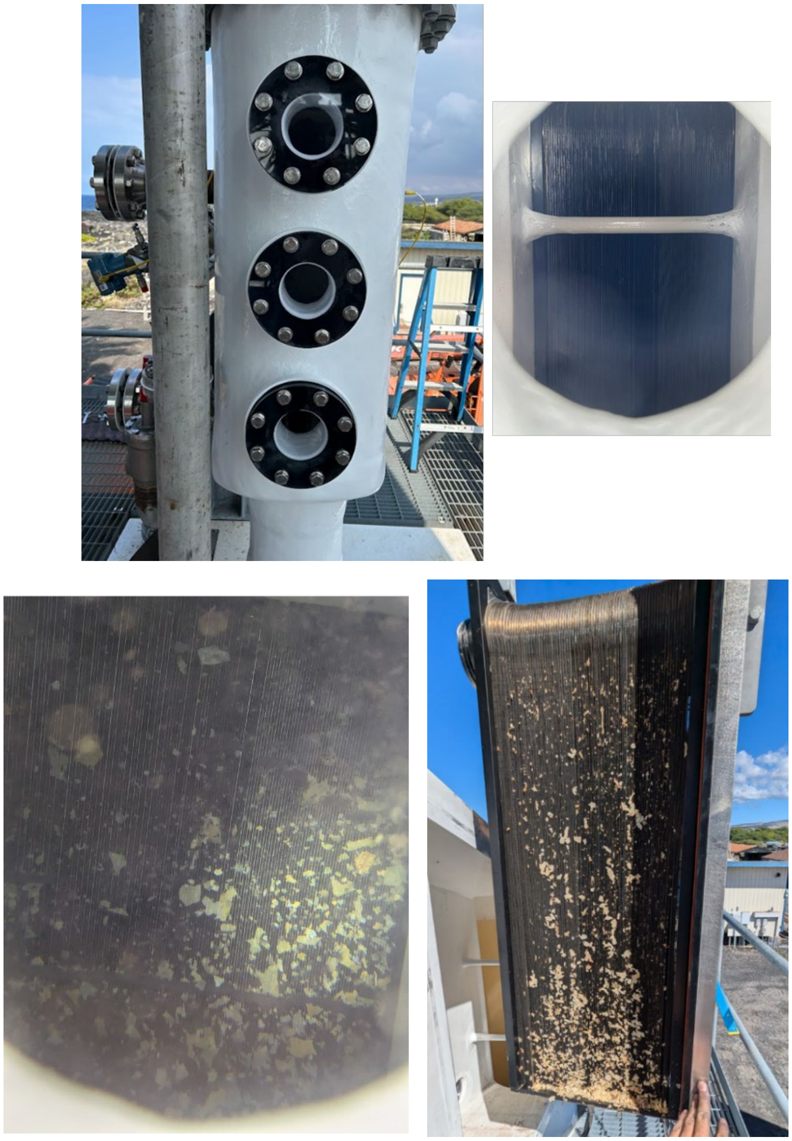

Figure 12. (top) View ports installed to monitor evaporator leading edge. (bottom) Debris from seawater piping system collected at the evaporator leading edge as seen through the viewport and when evaporator was removed for cleaning.

Future operations will use a sump pump when the intake strainer needs to be emptied. This effort prevents debris falling into the bottom of the piping during strainer removal. Makai also lined the strainer with a finer mesh screen so less debris can pass through the strainer.

3.1.4. Seawater Operations

Two key events highlighted the importance of establishing a procedure to operate and monitor the seawater system.

Makai previously established that the TFHXs must be flooded with seawater prior to being placed into ammonia service. This is for safety and because the cassette, housing, and hardware was designed to have seawater pressure counteracting some of the internal ammonia pressure. When seawater priming was lost following emergency system testing, the condenser began to slowly drain. Once priming was lost, cold seawater was no longer flowing to cool the condenser or the buffer tank. Ammonia temperature (and pressure) increased to ambient conditions (30°C, 1166 kPa) and the condenser stack began to leak. Makai attributes the leak to several compounding factors: the condenser experienced plate shift but was still sealed so the condenser was not removed to fix the plate shift; the manifold bolts were bent due to the plate shift event; there was no longer seawater pressure acting on the plates; the ammonia pressure was high, although not to the point of lifting a relief valve. The shifted stack was clearly misaligned in the center and this likely reduced the safety factor for maintaining compression and the TFHX experienced a leak at the center of the stack (Figure 13).

Figure 13. White residue at the center of the stack is indicative of an ammonia leak.

In addition to implementing automatic priming to maintain seawater priming, the control program will send alerts if seawater priming is lost or if based on flow and pressure measurements, the seawater side is draining/drained.

A separate incident occurred as the result of an upstream user at NELHA. After running high flow rates (~6,000 gpm) of warm seawater, flow was instantly stopped by shutting a valve. Makai's HX Test Facility is typically open/connected to the NELHA system (i.e., warm and cold seawater inlet valves are open). Because the NELHA pumps cannot respond instantaneously, the sudden stop by the upstream user produced a pressure transient that sheared off the top part of the FRP inlet strainer housing to Makai's HX Test Facility.

Figure 14. Top part of the strainer sheared off.

Makai personnel were on site and able to manually close an upstream valve to stop seawater from flooding the area. In addition to severing the strainer housing, the TFHX evaporator was also damaged. After removing the evaporator, pinhole leaks in the transition zone were found on several plates. Makai observed dents in the foil at the leak locations that are likely from debris that was wedged in between the plates. Makai suspects the evaporator had experienced multiple pressurization pulses since placed in service and debris was worked in between the plates during each cycle. Ultimately, one major event led to leaks in several plates.

Figure 15. TFHX evaporator showing residue from ammonia leak and debris around the manifolds.

Makai replaced the damaged plates, re-stacked and re-installed the evaporator. The strainer body required extensive fiberglass work but has been repaired. This event has emphasized the importance of serviceability of the cassette concept and the TFHX.

For future operations, Makai has communicated the importance of gradual decreases in seawater flow and is evaluating the tradeoffs in our procedures to shut the inlet to the facility when not in operation. This is not a preferred solution for the cold seawater because we cannot maintain flow to cool the condenser and the ammonia system. However, this has become our standard procedure to protect the warm seawater system. Alternatives include more rigorous review of tenant system designs prior to connection/operation with the NELHA seawater system.

3.2. SEAWATER-AMMONIA PERFORMANCE TESTING

Two 2-MW_{th} TFHXs, one evaporator and one condenser, were constructed under separate work and installed in the HX Test Facility (Table 3-1). Designs were selected based on 100-kW test data and Makai's OTEC model predictions. The evaporator was tested as a single-cassette unit and as a two-cassette unit by adjusting the ammonia liquid inlet valve to the second cassette. The condenser was tested as a two-cassette unit only. The evaporator was tested in a vertical, crossflow, falling film configuration and the condenser was tested in a horizontal, counterflow configuration (Figure 16). In addition to reporting the performance of each unit, comparisons to past performance (of the same design) helps characterize how results from small-scale testing translate to full-scale performance.

Table 3-1. Overview of TFHX test units.

	# Plates	Plate Spacing [mm]	Foil Thickness ["]	Internal Channel Size [mm]	Ammonia Path Length [m]	External Channel Size [mm]	SW Path Length [m]	HX Area [m^2]
Evaporator Single-Cassette (TFHX-1CAS-AC)	152	2.12	0.005	0.52	0.86	1.35	0.285	72.9
Evaporator Two-Cassette (TFHX-2CAS-AC)	304	2.12	0.005	0.52	0.86	1.35	0.57	145.9
Condenser Two-Cassette (TFHX-2CAS-AA)	304	2.12	0.005	0.68	0.86	1.19	0.86	145.9

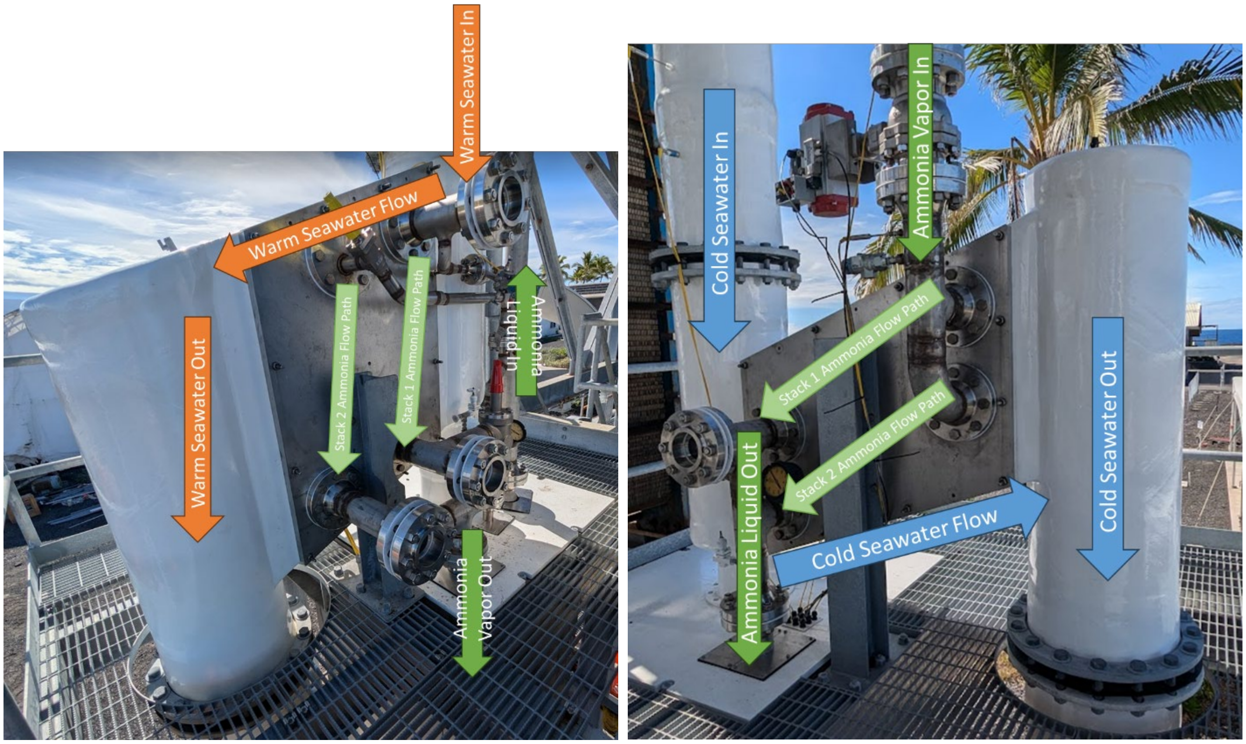

Figure 16 (left) Vertical, crossflow, falling film configuration for the evaporator. (right) horizontal, counterflow configuration for the condenser.

An initial set of performance data was collected on the TFHX condenser and evaporator. More extensive testing was planned but due to challenges with the ammonia pumps, coordinating water usage between tenants, and the strainer failure, additional testing will have to be conducted as part of future tasking.

3.2.1. Seawater Pressure Drop

Seawater-side pressure drop is related to the pumping power required to provide a certain seawater flow rate through the heat exchanger. The seawater pressure drop is mainly dependent on channel size and seawater velocity (Figure 17).

Evaporator seawater pressure drop vs flow lined up with previous data when corrected for the new seawater path length. For the condenser, the current pressure drop is up to 15% higher than previous data; there was also a 7% discrepancy in the previous data between FL4 and FL5 even though the channels were designed to be the same.

The discrepancy in the condenser is most likely attributed to uneven plate spacing. The condenser was assembled first and there was a clear sag in the middle. Because the condenser was pressurized and leak checked in place, there was some permanent deformation and the seawater channels were visibly uneven.

The evaporator assembly benefited from the lessons learned during condenser assembly. Spacer blocks were used between each plate to maintain the correct spacing and support the weight of the stack; as a result, the seawater channels in the evaporator are even (by visual inspection). The evaporator was restacked twice, once after the plate shift incident and most recently after the seawater pressure transient. Comb spacers were installed after the plate shift to aid in keeping the channels even and mitigate the debris that could work its way in between the plates.

Although the condenser was restacked using spacers after the leak due to loss of seawater priming / cooling, the plates were already warped and the channels were still visibly uneven. Comb spacers were not installed in the condenser, although, in the next iteration, comb spacers (or comparable method) will be added to aid in maintaining the seawater channel spacing.

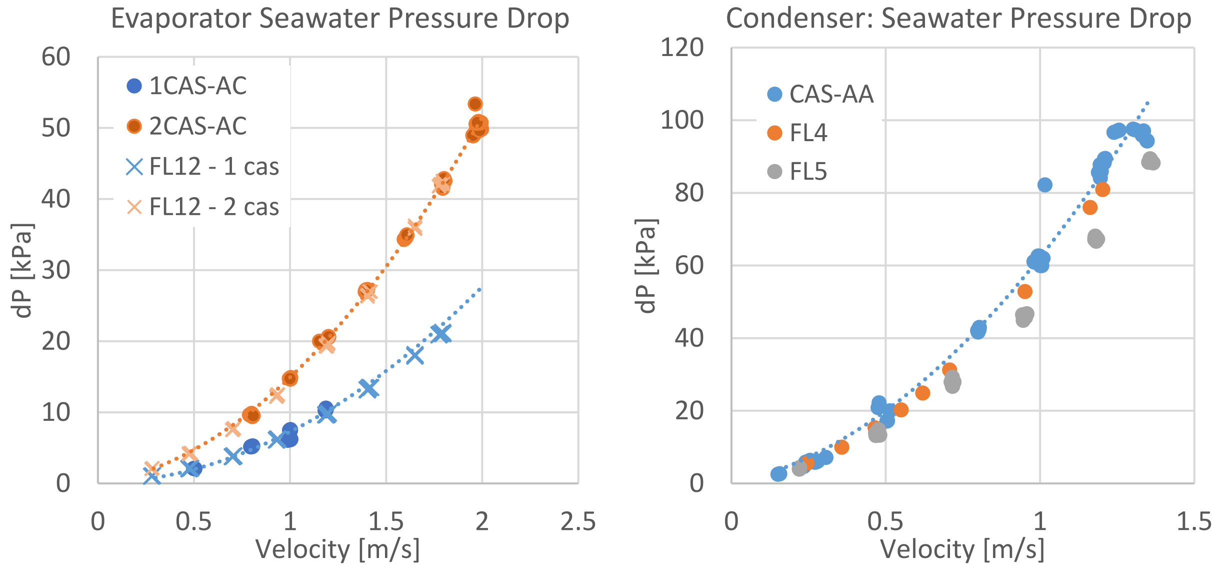

Figure 17. Seawater pressure drop.

3.2.2. Ammonia Pressure Drop

The ammonia flow path in the evaporator and condenser are different than previously tested configurations. In the 2-MW$_{th}$ evaporator, liquid ammonia is pumped to the top of the evaporator and vapor exits from the bottom. The previous 100-kW evaporator had liquid ammonia entering the bottom manifold and ammonia vapor exiting the top manifold. The 2-MW$_{th}$ condenser is oriented horizontally (at a 6° angle) with ammonia vapor entering the upper manifold and ammonia liquid exiting the lower manifold. The previous 100-kW condenser was oriented vertically, with ammonia vapor entering the top manifold and ammonia liquid exiting the bottom manifold. However, the ammonia path length is the full length of the plate in the 2-MW$_{th}$ evaporator and condenser, same as the previously tested 100-kW units.

At the same energy density, pressure drop was lower in the single-cassette test compared to the two-cassette test. This is most likely because the averaged energy density for the entire unit is reported whereas the actual energy density is likely higher in one cassette compared to the other. Compared to the 100-kW test, the pressure drop is lower in both single- and two-cassette evaporator tests. This is attributed to the lack of static head in the falling film configuration where ammonia liquid enters from the top versus the previous forced convection configuration where ammonia liquid enters from the bottom. Due to issues with the recirc pump, quality was difficult to control, particularly for the two-cassette testing. There is a substantial range in pressure drop, likely varying with quality, at each energy density. In the single-cassette test, for the same energy density, lower quality points had higher pressure drops whereas in the two-cassette testing, there is no clear trend. However, the reported quality is averaged between the two cassettes and individual quality in a single cassette may be different and account for the variation.

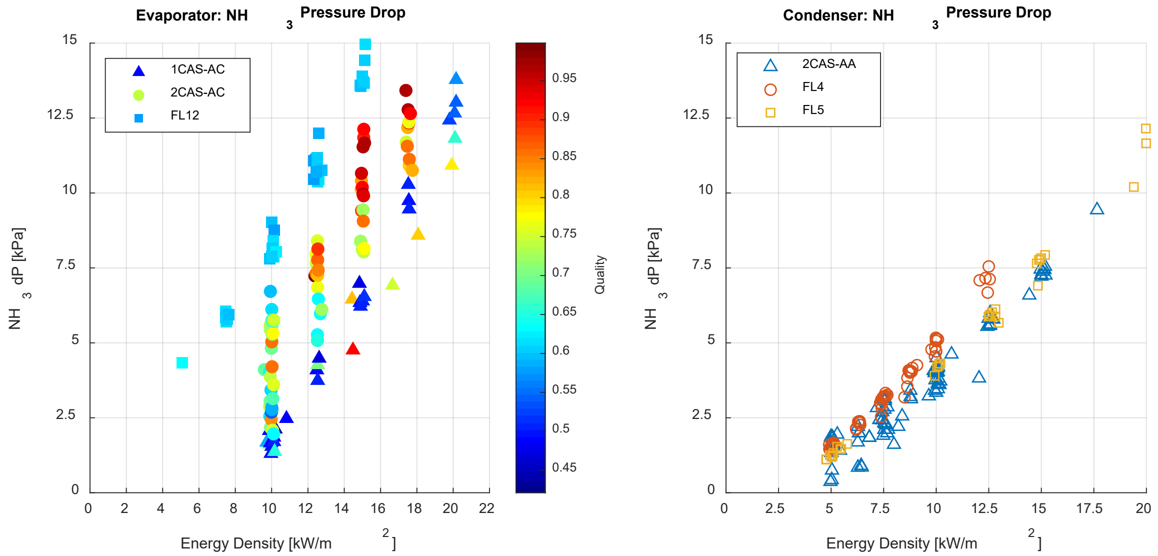

Figure 18. Ammonia pressure drop.

In the condenser, the ammonia pressure drop was either slightly lower or comparable to the previously tested 100-kW units (FL4 and FL5).

3.2.3. Overall Heat Transfer Coefficient

The overall heat transfer coefficient, U-value, is calculated using:

$$U = \frac{Duty}{Area \times LMTD}$$

where $LMTD = \frac{(T_{SW,in} - T_{sat\,NH3,out}) - (T_{SW,out} - T_{sat\,NH3,in})}{\ln \frac{(T_{SW,in} - T_{sat\,NH3,out})}{(T_{SW,out} - T_{sat\,NH3,in})}}$.

In the crossflow configuration, there is a correction factor, but based on the evaporating test conditions and configuration, the factor is close to 1.

For the condenser, U-value is dependent on seawater flow and energy density. In previous 100-kW testing, U-value did not vary much with energy density. In the current condenser, increasing energy density from 5 kW/m^2 to 15 kW/m^2 *increased* U-value 20-30% (e.g., from 3 kW/m^{2}K to 3.9 kW/m^2/K at 1.2 m/s). However, compared to 100-kW results, the U-value of the current condenser is ~40% lower than expected (e.g., 2.7 kW/m^2/K in 2CAS-AA compared to 4.5 kW/m^2/K in FL4 at seawater velocity of 0.8 m/s and energy density of 10 kW/m^2).

Since the ammonia pressure drop aligned with prior data but the seawater pressure drop did not, Makai suspects the seawater flow was not evenly distributed between the plates. If the seawater channels were “paired” (i.e., one larger channel and one smaller channel due to the warping of the plates), this could imply about half the plates received little seawater flow, and therefore, was effectively not contributing to heat transfer and reducing the effective area. Makai plans to construct and test a new condenser, using the spacers bars during stacking and comb spacers during operation to maintain even seawater channel spacing, to verify the less-than-expected performance was due to uneven channel spacing and not due to the horizontal orientation or issues with scaling from 100-kW test results.

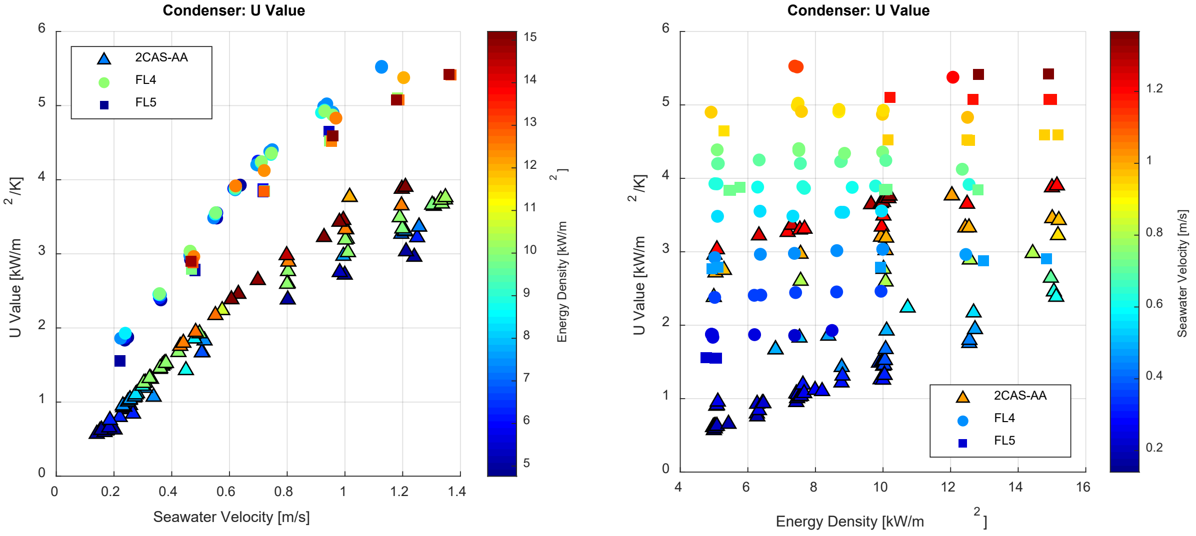

Figure 19. Condenser U-value varies with seawater flow and energy density.

For the evaporator, U-value is dependent on seawater flow rate, duty, and quality. In general, increasing velocity increased U-values. In the single cassette test, quality was maintained ~50% for all test points. Increasing energy density from 10 kW/m^2 to 20 kW/m^2 *decreased* the U value 10% (e.g., 5.7 kW/m^2/K to 5.2 kW/m^2/K at 1.2 m/s). In previous FL12 data where quality was maintained at 65%, increasing energy density from 10 kW/m^2 to 17.5 kW/m^2 *increased* U value 10% (e.g., 3.9 kW/m^2/K to 4.3 kW/m^2/K at 1.2 m/s).

In the two-cassette testing, at the same velocity increasing the quality from 60% to 98% *decreased* the U-value 28% (e.g., from 5 kW/m^2/K to 3.6 kW/m^2/K at 1.2 m/s). A separate variable that was not well captured in the initial testing was the distribution of duty between each cassette. During testing, Makai observed the U-value could be increased/decreased by adjusting the ammonia inlet valve to the first cassette. This changes both the quality distribution and the duty distribution between the two cassettes.

Makai installed temperature sensors to measure seawater temperature at the inlet, in three locations after the first cassette, and in the discharge piping after both cassettes. During single-cassette testing, there was some discrepancy between seawater duty calculated from the three temperature sensors immediately after the first cassette and ammonia duty. Because the evaporator is in a crossflow configuration, it is likely duty distribution is not evenly divided into thirds and a straight average of the temperature sensors may not accurately reflect duty. Makai intended to use the seawater duty to determine how duty is distributed between the two cassettes, but additional testing is needed to more accurately weight the temperature sensor measurements.

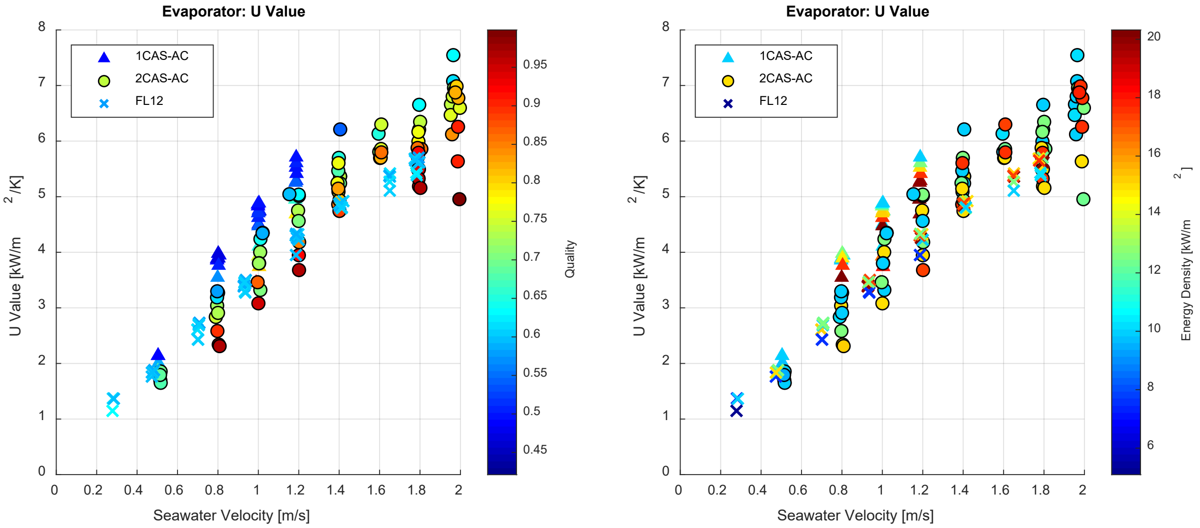

Figure 20. Evaporator U values increase with increasing seawater flow, but are also affected by energy density and quality.

Makai installed an orifice flow meter to measure ammonia flow into the first cassette and intended to use the total flow rate out of the recirc pump minus the flow rate entering the first cassette to calculate ammonia flow into the second cassette. However, the falling film configuration appears to favor higher qualities and ammonia flow rates were often above the range of the orifice flow meter. Instead, the flow rate into the first cassette will have to be calculated by correlating the pressure drop between the recirc pump discharge and first cassette inlet with flow rates maintained in range during single cassette operation.

Once duty and ammonia liquid flow rates in each cassette are resolved, the ammonia enthalpy at the outlet can be calculated using the duty, ammonia flow rate, and ammonia enthalpy at the inlet. Finally, the ammonia outlet enthalpy and outlet pressure can be used to estimate the outlet quality.

Due to delays required to repair the ammonia pumps and the extensive damage to the seawater strainer here was not enough time during this testing period to collect the data required to accurately characterize the duty and ammonia flow rates to analyze the duty and quality in each cassette. This task will be reserved for future testing.

3.2.4. Heat Exchanger Approach Temperature

Heat exchanger approach temperature is determined by the seawater temperature, seawater flow rate, and duty. Makai is defining the approach temperature as:

$$T_{approach} = T_{warm\ seawater\ in} - T_{saturation\ at\ EOPS}\ \text{(evaporator)}$$

$$T_{approach} = T_{saturation\ at\ CIPS} - T_{cold\ seawater\ in}\ \text{(condenser)}$$

Makai's definition is customized for OTEC purposes; the ammonia saturation temperatures at the evaporator outlet and condenser inlet are used because these are directly connected to the turbine inlet/outlet. Additionally, because the bulk of the duty is in phase change, superheating at the condenser inlet is not accounted for and the saturation temperature is used instead of the measured temperature.

For OTEC operations, small approach temperatures result in higher available differential pressure across the turbine. Higher seawater flow rates yield smaller approach temperatures, but also require higher parasitic losses from high volumetric flow rates and/or high seawater pressure drops.

The focus of performance testing was to determine whether predicted results using 100-kW test data would translate to the 2-MW$_{th}$ scale. Admittedly, although the plate design is the same, the evaporator configuration is substantially changed by going from counterflow to crossflow and forced convection to falling film on the ammonia side.

One way to compare heat exchanger performance is to plot the approach temperature versus energy density and pumping power through the heat exchangers (for the same heat exchanger area, Figure 21 and Figure 22).

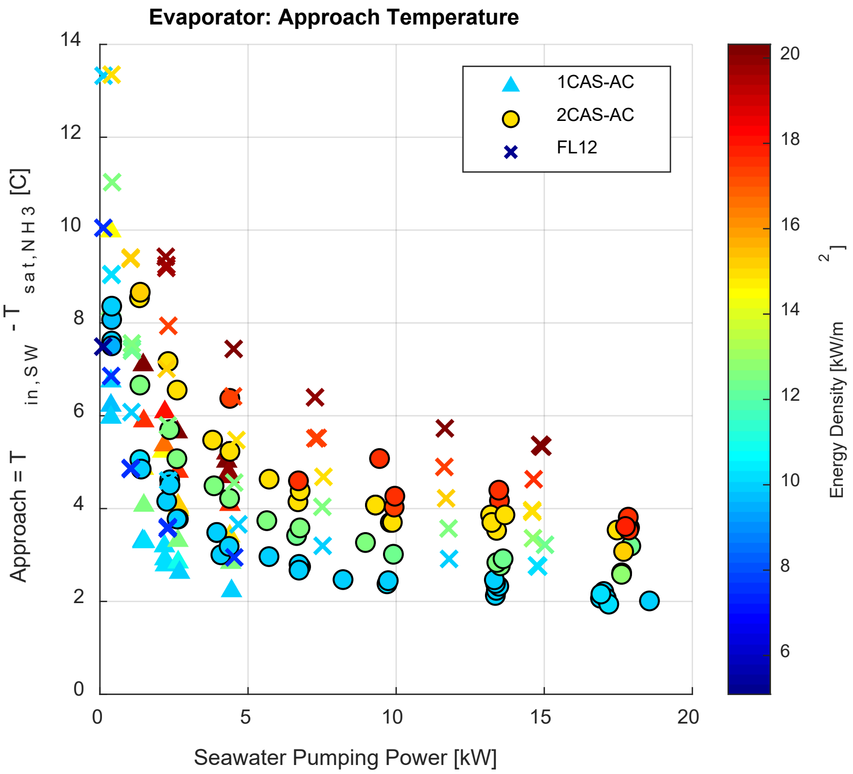

Figure 21. Evaporator approach temperature.

While the single-cassette unit had the lowest approach temperature, it is not the most practical design because the seawater path is short and in order to meet the required duty, arranging all the units would require a lot of frontal area (and a larger system size). The two-cassette unit had the same as or better approach temperatures compared to FL12. Makai also expects slight improvement in two-cassette performance if higher qualities could be tested, particularly at high energy densities.

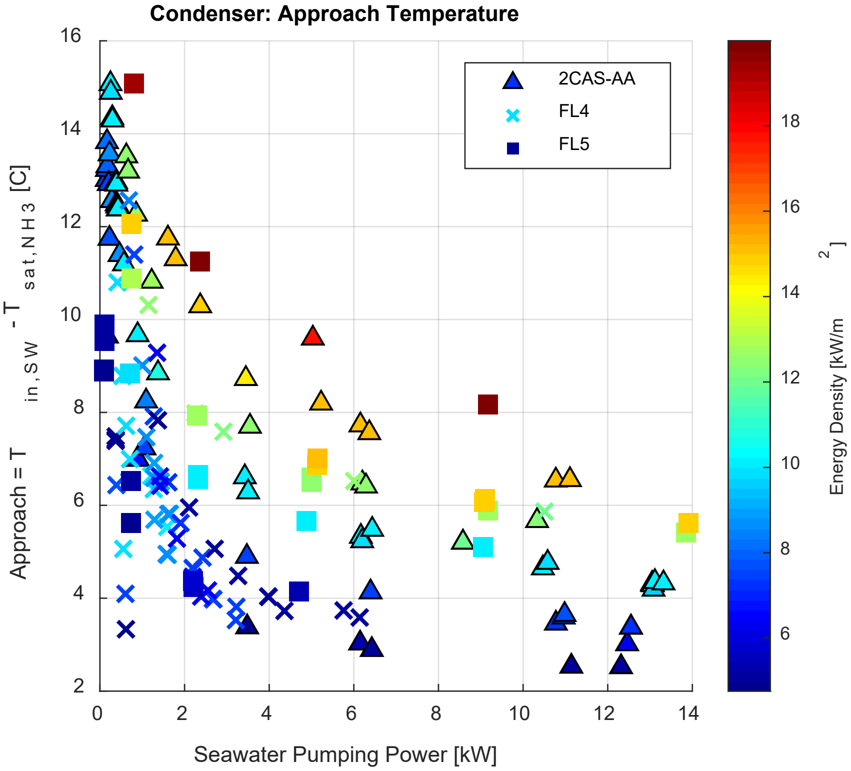

Figure 22. Condenser approach temperature.

The condenser approach was higher than both FL4 and FL5 at lower pumping powers but comparable at higher pumping powers. This result is not unexpected based on the mismatch in seawater pressure drop and U-values.

This analysis only considers the pumping power through the heat exchanger. For OTEC operations, the total volume of seawater flow is also important, particularly for the condenser due to losses in the cold water pipe. A comprehensive comparison of TFHX designs in the OTEC context will require a tradeoff study evaluating increase in net power production gained by smaller approach temperatures versus a larger cold water pipe and overall OTEC system (i.e., more expensive capital investment).

3.3. DISCUSSION

Makai previously reported on the development of the OTEC Power Calculator, a tool to evaluate different heat exchanger designs in the context of an OTEC system performance. Heat exchangers can be compared in terms of area (i.e., heat exchanger cost) or volume (i.e., system size and cost) required to produce a targeted net power. The calculator takes into account seawater flow rates through the heat exchangers *and* the system (cold water pipe, intake screen, discharge pipe).

Makai previously compared heat exchanger designs by setting the heat exchanger area and seawater temperature and varying seawater flow rates and turbine parameters to maximize net power. The best combination used FL-12 and FL-5 as the evaporator and condenser, respectively.

For the evaporator, a 1:1 area replacement of FL-12 with the two-cassette unit produces ~10% less gross power and 7.5% less net power. This is because the two-cassette unit is oriented the crossflow configuration and at the same volumetric flow rate, the velocity through the heat exchanger is lower (because the cross-section flow area is larger in crossflow). Increasing the flow rate produces more power (gross and net) but requires larger ducting to manage the volume at reasonable pressure drop. Without increasing the ducting, the increase in parasitic losses exceeds the gains in gross power. This also means by increasing the volumetric flow rate and ducting size, the same net power can be achieved with less heat exchanger area.

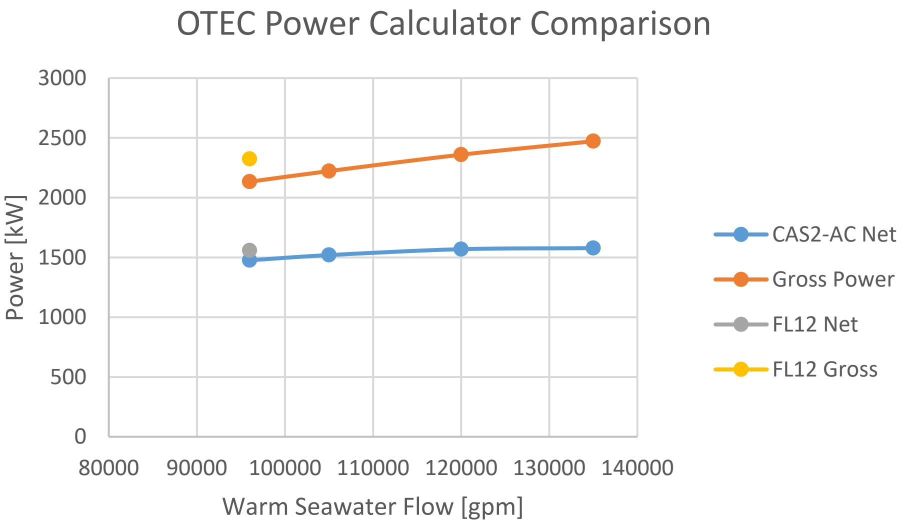

Figure 23. For the same area, the two-cassette unit requires higher seawater flows (and increasing duct size) to match net power.

Based on the U-value and seawater pressure drop results, the condenser was not expected to match predictions based on FL4 / FL5 results. This was confirmed in the OTEC power calculator. For the same area, CAS2-AA produced 10% less gross power and 20% less net power. Makai attributes the poor performance to the uneven seawater channels and will validate once a new condenser can be constructed and tested.

4. PROTOTYPE DESIGN

4.1. CASSETTE DESIGN FOR COMMERCIAL SEAWATER-COOLED HEAT EXCHANGER (TFPX)

Makai continues to focus on developing a heat exchanger unit that has a clear path to commercialization. Makai is focusing on seawater-cooled applications to take advantage of the TFHX's titanium, corrosion resistant construction, and serviceability.

Makai previously developed pipe (TFPX), tank (TFTX), and modular concepts to contain the external fluid and "house" the TFHX plates. In all three concepts, TFHX plates are installed as cassettes, which means the plate stack remains in compression during removal/installation.

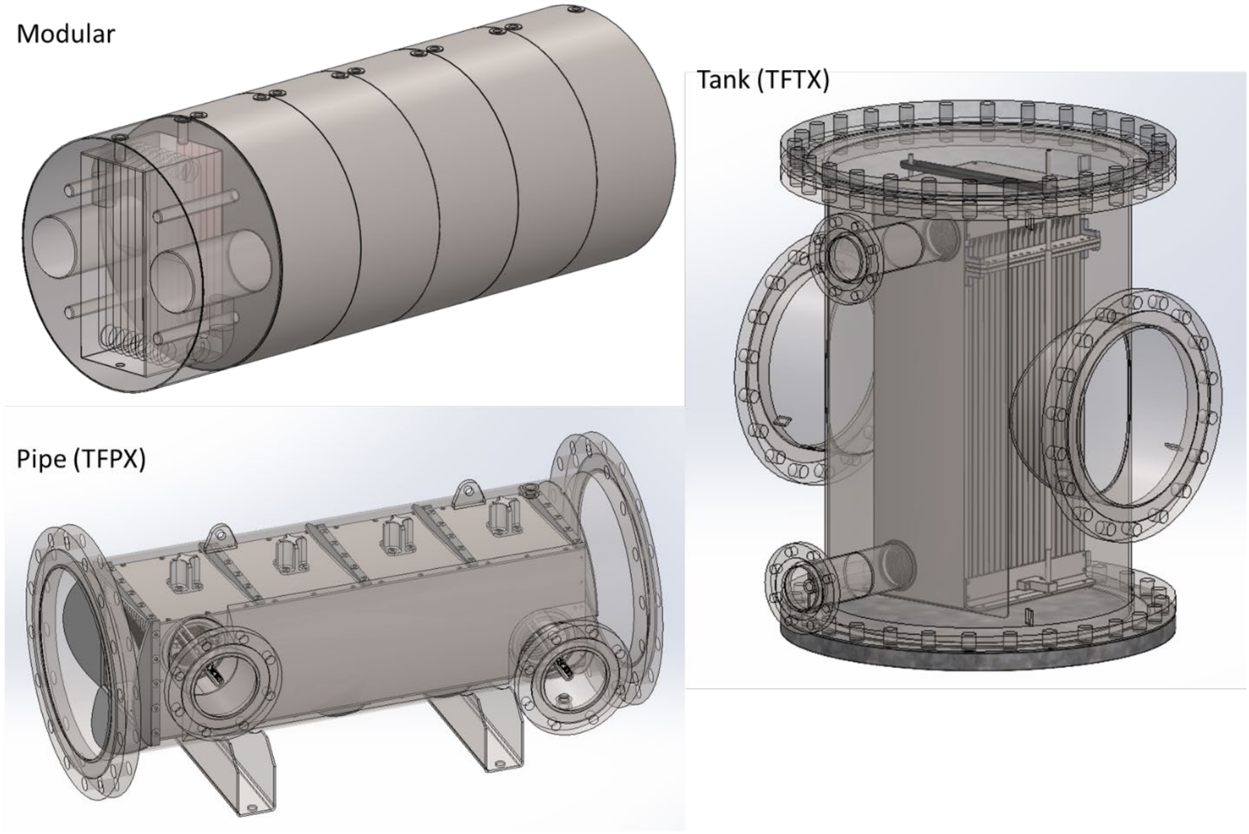

Figure 24. Modular, Tank, and Pipe concepts.

Early concepts for the TFTX had a removeable cover so the plate stack could be accessed in place and the internal fluid path could remain sealed/intact. However, more detailed review identified complexities and losses in the external flow path and based on ROM quotes, the concept was not cost effective. A modified design eliminated the expensive components but the cassette would no longer be accessible in place.

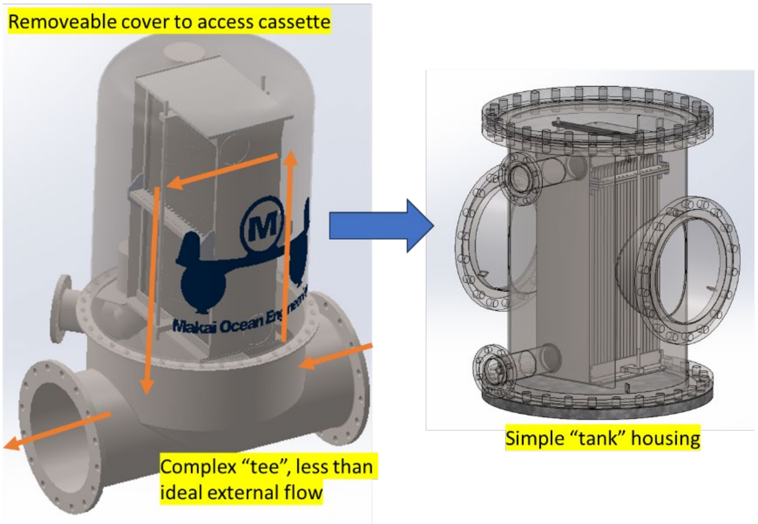

Figure 25. Tank concept progression.

After comparing the concepts, Makai selected the TFPX to proceed with prototype construction and testing. The TFPX is more cost effective for small (single-cassette) units and, without in-situ cleaning, the TFPX can be arranged in a counterflow configuration which is advantageous for water/water performance.

The first TFPX unit is designed to use a 130-plate cassette that fits in an 18” pipe. The unit can be installed horizontally or vertically. The housing is designed such that the cassette slides in until it hits a stop which aligns the internal manifolds with the internal fluid flange connections on the housing. The stop also serves as a flow blocker so external flow passes through the cassette rather than around it. Flow guides at the inlet face also aid in directing flow into the cassette.

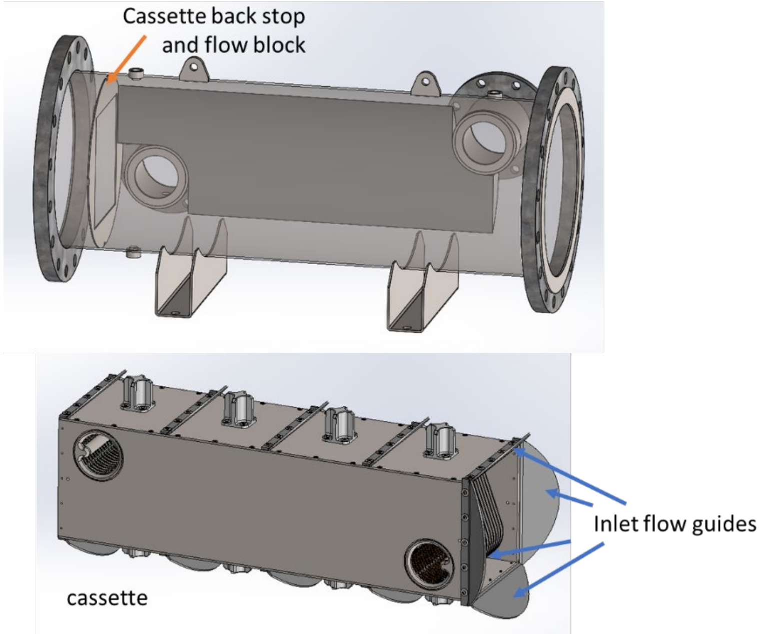

Figure 26. TFPX housing and cassette.

Makai envisions a vertical installation for the TFPX even if it is mounted horizontally for operations. Makai’s current in-situ cleaning methods are not compatible with counterflow configurations; for servicing, the unit will have to be removed from the piping system prior to removing the cassette. As Makai continues biofouling control research, future versions of the TFPX may include in-situ cleaning in the counterflow configuration.

5. BIOFOULING

Untreated, biofouling can have a detrimental impact on heat exchanger performance by increasing the pressure drop through the heat exchanger and decreasing the heat transfer performance. In this period, Makai completed 1-year testing of a baseline and automated cleaning system. Makai continued submerged biofouling test with automated brushing.

5.1. AUTOMATED CLEAN-IN-PLACE

After one year of operation, the automated clean-in-place prototype (ACIP) experienced only 13% increase in pressure drop compared to the baseline (no cleaning) test which had over 400% increase in pressure drop (Figure 27). A portion of the increase in pressure drop in the ACIP is attributed to the surfaces that are not cleaned. Based on visual inspection, the plates were generally clean. There was soft and hard fouling on edges of the plates; hard fouling was predominantly at the leading and trailing edge seal welds.

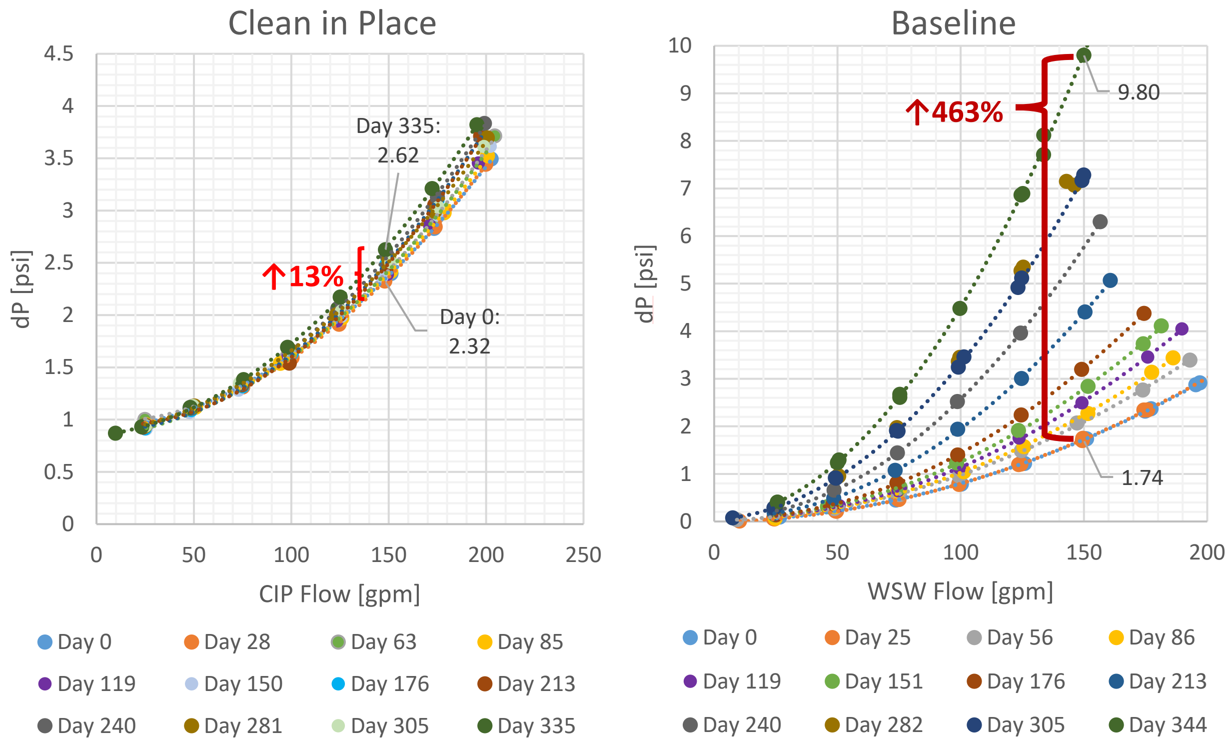

Figure 27. Baseline test shows >400% increase in pressure drop after almost 1 year. The clean-in-place sample has ~13% increase in pressure drop over the same period.

5.2. SUBMERGED BIOFOULING TEST

Makai has two submerged biofouling tests in operation. Periodic visual inspections are used to assess performance.

5.3. INTAKE SCREEN TESTING

As observed during evaporator testing, the compact channels of the TFHX are susceptible to clogging from debris. Makai has been testing a self-cleaning intake screen by ISI, Inc (Figure 28) for one year. The test is to determine the efficacy of the cleaning mechanism, understand the required maintenance cycles, and evaluate the durability of the components in order to understand where improvements are needed for long-term deployment.

The discoloration on the screen is fouling that is easily removed with a brush. Makai has observed that the screen is not perfectly round and the screen bristles do not evenly make contact across the entire surface of the screen. There has been no corrosion observed on the screen. The anode surface was cleaned twice, at about 3 and 6 months after installation and replaced at 10 months (Figure 29).

Figure 28. (top) Intake screen upon installation. (bottom) Intake screen after one year.

Figure 29. Old (left) and new (right) anode.

6. SUMMARY

Between November 2024 – July 2025, Makai designed the next generation TFHX plate fabrication equipment; commissioned the new HX Testing Facility; performance tested two cassette-style 2-$MW_{thermal}$ TFHXs; developed concepts for large-scale seawater-water TFHXs; and prototyped new biofouling mitigation methods.

TFHX Design and Fabrication. Makai validated the cassette-style design by uninstalling and reinstalling both the condenser and evaporator several times. The cassette-style design enabled smooth and quick installation and removal.

Makai tried form-in-place (FIP) gaskets to improve the assembly process but the gaskets were incompatible with ammonia. Because the gaskets require substantial equipment investment, Makai is currently not considering the FIP gaskets even for non-ammonia applications.

Makai constructed a single plate, internal pressure drop test station to aid in designing plates for applications where water (or similar) is the internal fluid. The current TFHX plate designs have small internal channels which are favorable when ammonia is used as the internal fluid. As expected, when using water as the internal fluid in the same designs, the pressure drop is higher than existing specifications for seawater cooled applications. With the single plate pressure drop test station, Makai can more effectively test and optimize designs for water as the internal fluid.

Makai also designed the next generation fabrication equipment which is expected to reduce plate fabrication time while improving the reliability and quality of the plate.

Prototype Design. For large-scale seawater-seawater/water applications, Makai selected the TFPX to proceed with prototype construction and testing. The 18”-TFPX will hold a 130-plate cassette containing 65 m^2 of heat transfer area. The first prototype will be arranged in a counterflow configuration without in-situ biofouling controls. This prototype is intended for performance demonstration and cassette servicing demonstration.

TFHX Performance Testing. In this period, Makai tested two 2-MW_{th} ammonia-seawater (OTEC) cassette-style TFHXs. The evaporator used the same plate design as the FL12 plates but was configured in a vertical, crossflow, falling-film orientation. In terms of U-value and approach temperature, performance was comparable to FL12 four-port TFHXs; however, because the crossflow orientation has a larger flow area, higher flow rates (and therefore, larger ducting) are required to match the net power produced in an OTEC system. The condenser used the same plate design as FL4 plates and was configured in a horizontal, counterflow orientation. Due to challenges during assembly, the plates were visibly warped and the seawater channels were visibly uneven; Makai suspects this was the root cause for the performance being lower than predicted based on FL4. Makai intends to retest the same condenser design after correcting the seawater channel spacing.

Biofouling. Makai de-commissioned the automated cleaning and baseline biofouling tests after one year. In the baseline test, the pressure drop increased 460% since Day 0 whereas in the automated cleaning test, pressure drop has only increased 13%. Makai has continued the submerged biofouling tests.

Upcoming Work

The major points of focus for Makai's near-term work are to:

- Retest the 2-$MW_{thermal}$ TFHXs to ground truth performance predictions based on 100-kW scale test data
- Continue to develop cost-effective designs for large-scale seawater-seawater/water applications
- Improve the speed and variability in TFHX plate fabrication time and success rate through automation to remove dependence on operator skill
- Continue to develop, prototype and test in-situ biofouling control/mitigation systems